

Supporting information

Conductive two-dimensional $M_3(C_6S_3O_3)_2$ monolayers as efficient electrocatalysts for oxygen reduction reaction

Tianchun Li,[†] Manman Li,[†] Xinyue Zhu,[†] Juan Zhang,[†] Yu Jing^{†*}

[†]Jiangsu Co-Innovation Centre of Efficient Processing and Utilization of Forest Resources, International Innovation Center for Forest Chemicals and Materials, College of Chemical Engineering, Nanjing Forestry University, Nanjing 210037, China

To whom correspondence should be addressed. Email: yujing@njfu.edu.cn(YJ)

Table S1 Lattice parameter, pore size and formation energy (E_f) of each $M_3(C_6S_3O_3)_2$ monolayer.

M	Co	Cr	Cu	Fe	Mn	Ni	Pd	Rh	Ru
Lattice (Å)	13.64	14.05	13.77	13.79	13.90	13.60	14.05	14.10	14.22
Dp (Å)	10.57	10.87	10.69	10.70	10.73	10.52	10.96	11.06	11.16
Dm (Å)	6.82	7.03	6.89	6.90	6.95	6.80	7.03	7.05	7.11
E_f (eV)	-14.22	-12.06	-6.11	-12.70	-12.41	-13.47	-8.24	-14.21	-18.20

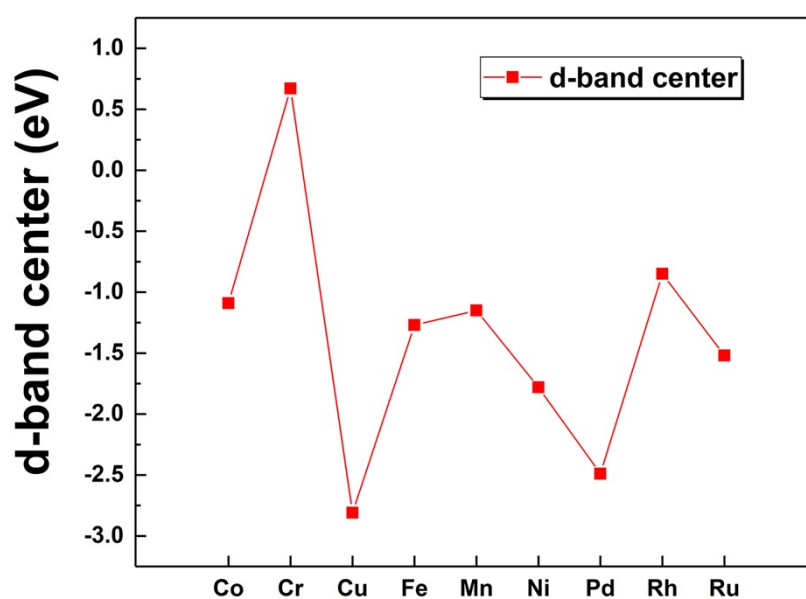


Fig. S1 The value of d-band center (ϵ_d) of transition metals of different $M_3(C_6S_3O_3)_2$ monolayers.

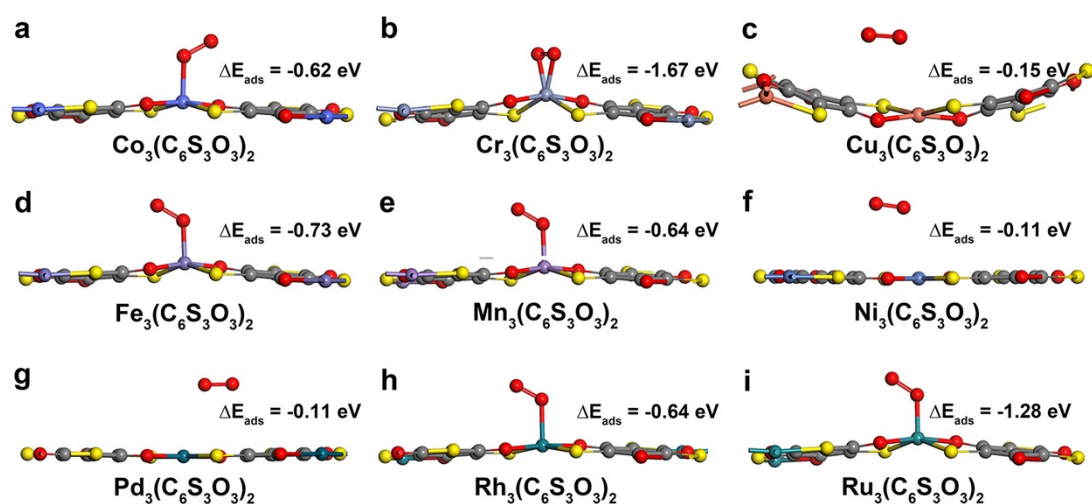


Fig. S2 Schematics of O₂ adsorption on M₃(C₆S₃O₃)₂ monolayers.

Table S2 Gibbs free energy change (ΔG) of each elementary step for ORR on M₃(C₆S₃O₃)₂ monolayers

M=	Co	Cr	Cu	Fe	Mn	Ni	Pd	Rh	Ru
ΔG_1 (eV)	-0.79	-1.66	0.05	-0.94	-1.00	0.09	0.24	-0.81	-1.80
ΔG_2 (eV)	-1.78	-3.12	-3.20	-2.23	-2.43	-3.12	-0.76	-1.67	-2.63
ΔG_3 (eV)	-1.34	-0.30	-0.58	-1.04	-0.79	-0.62	-2.19	-1.48	-0.46
ΔG_4 (eV)	-1.00	-0.16	-1.19	-0.71	-0.70	-1.27	-2.21	-0.96	-0.03

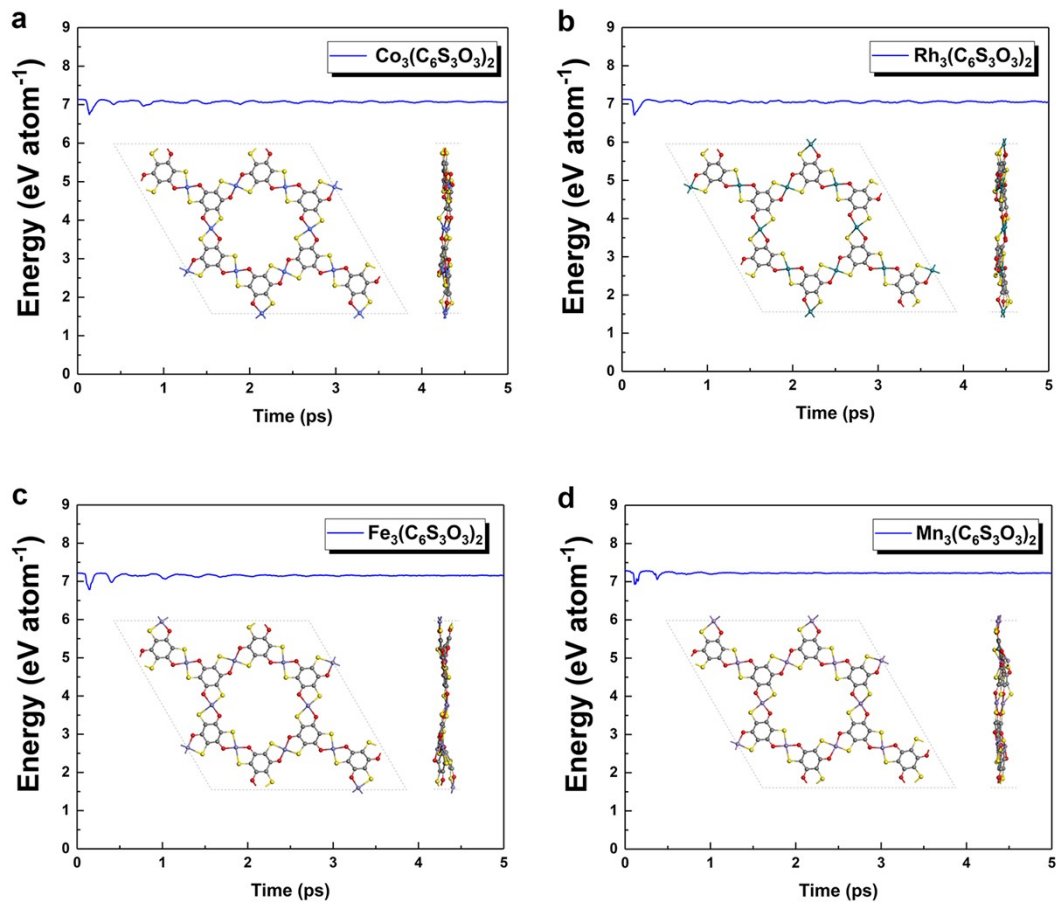


Fig. S3 The change of total energy with time for (a) $\text{Co}_3(\text{C}_6\text{S}_3\text{O}_3)_2$, (b) $\text{Rh}_3(\text{C}_6\text{S}_3\text{O}_3)_2$, (c) $\text{Fe}_3(\text{C}_6\text{S}_3\text{O}_3)_2$, and (d) $\text{Mn}_3(\text{C}_6\text{S}_3\text{O}_3)_2$ monolayer by *ab initio* molecular dynamic (AIMD) simulations at 500 K for 5 ps. Inside are top and side views of $\text{Co}_3(\text{C}_6\text{S}_3\text{O}_3)_2$, $\text{Rh}_3(\text{C}_6\text{S}_3\text{O}_3)_2$, $\text{Fe}_3(\text{C}_6\text{S}_3\text{O}_3)_2$, and $\text{Mn}_3(\text{C}_6\text{S}_3\text{O}_3)_2$ monolayer at $T=500$ K after 5 ps.

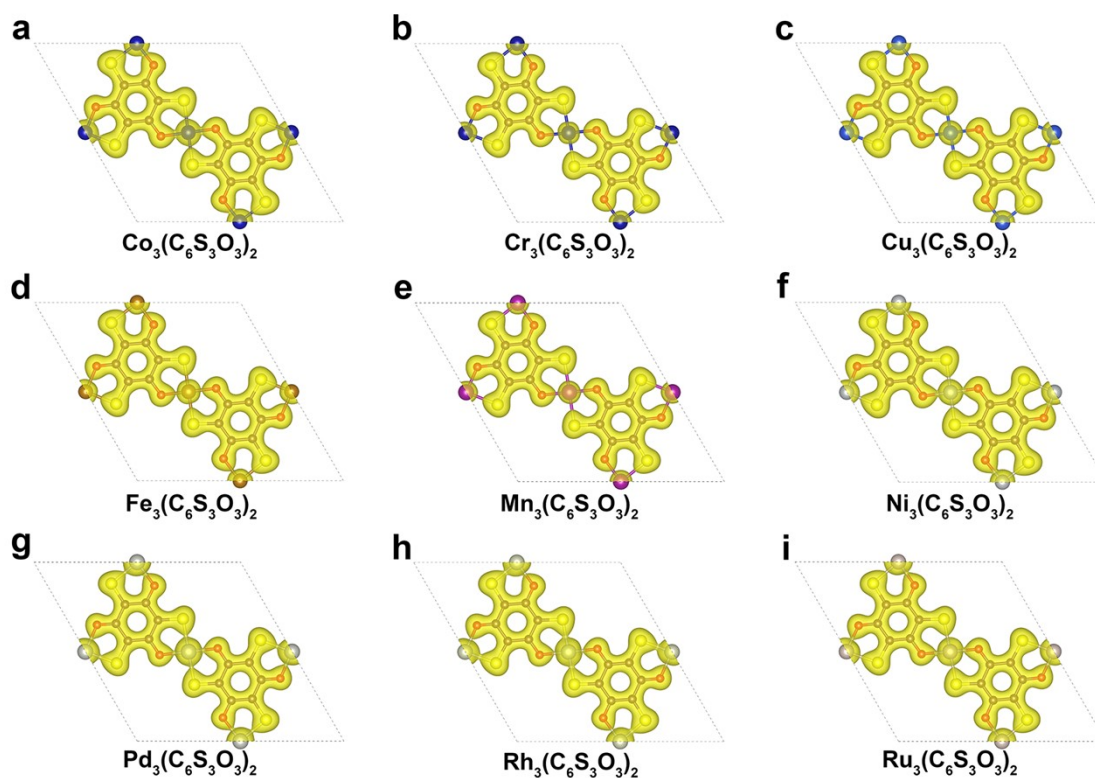


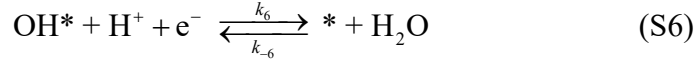
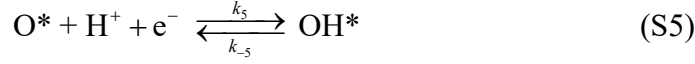
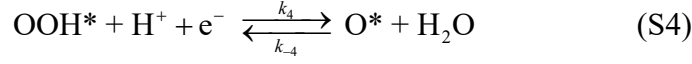
Fig. S4 The charge density distribution of $M_3(C_6S_3O_3)_2$ monolayer. The isosurface value is set to be $0.1 e/\text{Bohr}^3$.

Table S3 Charge ($|e|$) transferred between central metal atoms and surrounding oxygen and sulfur atoms of the MS_2O_2 moieties.

	M	O	S
$Co_3(C_6S_3O_3)_2$	-0.86	1.00	-0.04
$Cr_3(C_6S_3O_3)_2$	-1.26	1.04	0.13
$Cu_3(C_6S_3O_3)_2$	-0.81	1.01	-0.04
$Fe_3(C_6S_3O_3)_2$	-1.08	1.01	0.06
$Mn_3(C_6S_3O_3)_2$	-1.28	1.04	0.11
$Ni_3(C_6S_3O_3)_2$	-0.77	0.98	-0.06
$Pd_3(C_6S_3O_3)_2$	-0.63	0.96	-0.10
$Rh_3(C_6S_3O_3)_2$	-0.63	0.96	-0.10
$Ru_3(C_6S_3O_3)_2$	-0.95	0.98	0.02

Details of microkinetics simulations

The polarization curve of the $M_3(C_6S_3O_3)_2$ monolayers was simulated based on a general kinetic model applicable to ORR.¹ The O_2 adsorption (non-electrochemical step) and electrochemical steps are listed below:



where k_i and k_{-i} denote the forward and reverse reaction rate constant, respectively. $O_2(\text{aq})$ and $O_2(\text{dl})$ refer to the O_2 in the electrolyte and catalyst-electrolyte interfaces, respectively.

According to the above elementary steps, the rate equation for each species can be expressed as:

$$\frac{\partial x_{O_2(\text{dl})}}{\partial t} = k_1 x_{O_2(\text{aq})} - k_{-1} x_{O_2(\text{dl})} - k_2 x_{O_2(\text{dl})} \theta^* + k_{-2} \theta_{O_2^*} \quad (\text{S7})$$

$$\frac{\partial x_{O_2^*}}{\partial t} = k_2 x_{O_2(\text{dl})} \theta^* - k_{-2} x_{O_2^*} - k_3 \theta_{O_2^*} + k_{-3} \theta_{OOH^*} \quad (\text{S8})$$

$$\frac{\partial x_{OOH^*}}{\partial t} = k_3 \theta_{O_2^*} - k_{-3} \theta_{OOH^*} - k_4 \theta_{OOH^*} + k_{-4} \theta_{O^*} \quad (\text{S9})$$

$$\frac{\partial x_{O^*}}{\partial t} = k_4 \theta_{OOH^*} - k_{-4} \theta_{O^*} - k_5 \theta_{O^*} + k_{-5} \theta_{OH^*} \quad (\text{S10})$$

$$\frac{\partial x_{OH^*}}{\partial t} = k_5 \theta_{O^*} - k_{-5} \theta_{OH^*} - k_6 \theta_{OH^*} + k_{-6} \theta^* \quad (\text{S11})$$

where x , θ and t refer to molar fraction, coverage of the species and time, respectively. x_{H_2O} is taken as 1 and $x_{O_2(\text{aq})}$ is taken as a value of 2.34×10^{-5} , denoting $O_2(\text{g})$ at equilibrium with $O_2(\text{aq})$ at 1 atm.

For the non-electrochemical step i , the equilibrium constant (K_i) and k_i can be expressed as:

$$K_i = \exp\left(-\frac{\Delta G_i}{k_B T}\right) \quad (\text{S12})$$

$$k_i = v_i \exp\left(-\frac{E_{a,i}}{k_B T}\right) \quad (\text{S13})$$

where ΔG_i is the free energy change of step i, v_i is the pre-exponential factor and $E_{a,i}$ is the activation energy. In addition, k_B is the Boltzmann constant and T is the temperature taken as 298.15K.

K_i and k_i for electrochemical step i, which is associated with both the electrode potential(U), can be calculated with the following equations:

$$K_i = \exp\left(-\frac{e(U-U_i)}{k_B T}\right) \quad (\text{S14})$$

$$k_i = A_i \exp\left(-\frac{E_{a,i}}{k_B T}\right) \exp\left(-\frac{e\beta_i(U-U_i)}{k_B T}\right) \quad (\text{S15})$$

where U_i is the reversible potential of step i derived from $U_i = -\Delta G_i / e$, A_i refers to the effective pre-exponential factor with a value of 1.23×10^9 , and β_i denotes the symmetric factor taken as 0.5.

Since the $E_{a,i}$ values of electrochemical steps of the ORR are usually small, in the range from 0.10 to 0.26eV,² $E_{a,i} = 0.26\text{eV}$ was employed for all the electrochemical steps of the ORR on the $\text{M}_3(\text{C}_6\text{S}_3\text{O}_3)_2$ monolayers.

Furthermore, for all the reverse reactions, the rate constants (k_{-i}) can be derived from the following equation:

$$k_{-i} = \frac{k_i}{K_i} \quad (\text{S16})$$

Finally, the current density(j) can be calculated according to the following equation:

$$j = e\rho TOF_e \quad (\text{S17})$$

1 H. A. Hansen, V. Viswanathan and J. K. Nørskov, *J. Phys. Chem. C*, 2014, **118**, 6706-6718.

2 V. Tripković, E. Skúlason, S. Siahrostami, J. K. Nørskov and J. Rossmeisl, *Electrochim. Acta*, 2010, **55**, 7975-7981.